VNU Journal of Science, Mathermatics – Physics 27 (2011) 204-211

Preparation of $NiFe_2O_4$ - TiO_2 nanoparticles and study of their photocatalytic activity

Do Quoc Hung*, Nguyen Kim Thanh

Le Quy Don Technical University, 100 Hoang Quoc Viet Street, Ha noi, Viet Nam.

Received 30 October 2011, received in revised form 24 November 2011

Abstract. In this article, the authors describe the method for preparation of $NiFe_2O_4$ – TiO_2 magnetic nanoparticles and present the results on study of their photocatalytic activity. $NiFe_2O_4$ nanoparticles have been prepared by coprecipitation using spraying technique with subsequent hydrothermal processing. $NiFe_2O_4$-TiO_2 composite nanoparticles were prepared by covering thin films of TiO_2 on the surface of $NiFe_2O_4$ particles using sol – gel technique. Different techniques such as XRD, TEM, SEM were used to characterize $NiFe_2O_4$ and $NiFe_2O_4$ – TiO_2 composite nanoparticles obtained from the mentioned procedure. It is shown that prepared $NiFe_2O_4$ – TiO_2 nanoparticles are particles of a composite material which consists of trevorite $NiFe_2O_4$ and anatase TiO_2 phases. TEM study has showed that the particles size is of about 20nm. The VSM measurement has demonstrated that nickel ferrite nanoparticles and $NiFe_2O_4$ – TiO_2 composite nanoparticles are superparamagnetic with saturation magnetization (Ms) of about 40 emu/g and 20 emu/g, respectively; remanences (Mr) and coercive forces (Hc) being near to zero for both the materials. The composite $NiFe_2O_4$ - TiO_2 nanoparticles are used to degrade methyl orange dye. After 14 hours, methyl orange with the initial concentration of 10^{-4}M is degraded 98,2%. Thanks to magnetic properties, the nanocomposite photocatalyst $NiFe_2O_4$ - TiO_2 can be easily collected for reuse.

Keywords: Magnetic nanoparticles, superparamagnetism, $NiFe_2O_4$-TiO_2 nanocomposite, photocatalysis.

1. Introduction

Magnetic nanoparticles of ferrites MFe_2O_4 (M : Ni, Mn, Zn, Cu...) recently attracted attention of many authors because they can be used for wide applications, such as high density information storage materials, ferrofluids, high frequency devices, magnetic refrigerants, gas- and biosensors [1, 2, 3]. Their advantages are high saturation magnetization, superparamagnetism, stability of properties at high frequencies, mechanical and chemical durability. Being semiconductors, spinel ferrites are also promising materials for spintronics [4]. On the other hand, TiO_2 is a well known semiconductor photocatalyst because of its capabilities of removing toxic organic and inorganic matters from the air and water environments as well as disinfection activity [5, 6, 11]. During treatment of wastewater with

* Corresponding author. Email: hungdq@mta.edu.vn

TiO_2, TiO_2 nanopowders can not be recovered, causing additional expense and problems of solid wastes, because filtering nanostructured TiO_2 is also a problem in the long-term water treatment. Fixation of TiO_2 photocatalyst on different supports as fibers, or zeolites could be a solution for this problem, but in this case the mobility of the catalyst is not high. If TiO_2 nanoparticles were embedded in the magnetic nanopowders, the problem of recovering TiO_2 for recycling and preventing environmental negative impacts can be resolved. Such magnetic nanocomposite materials containing TiO_2 will have high mobility, large contact area with wastewater, which will increase environment treatment efficiency, and they can be easily recollected by using an external magnetic field. Magnetic particles, which play the role of a photocatalyst carrier, must be nontoxic and stable in the environment. For the mentioned reasons, in this research, we have chosen nanocomposite powder $NiFe_2O_4 – TiO_2$ as the object of our study.

2. Experiment

2.1 Process of synthesizing nanostructured $NiFe_2O_4$

Diagram of experimental procedure for synthesis of nickel ferrite nanopowders and schema of apparatus for co-precipitation reaction are shown in Fig. 1.a and Fig. 1.b, respectively. Liquid mixture of solutions $NiCl_2$ 0.1 M + $FeCl_3$ 0.2 M prepared from $NiCl_2.4H_2O$ and $FeCl_3.6H_2O$ is contained in the 10 liter pressure vessel (2). The 10 liter pressure vessel (3) contains the solution NaOH 0.8 M. A flow of compressed air is blown through the pipe (1) into the two vessels so that the liquids come out of two containers in the mist form at the nozzles (4) and (5). Spray speed at the two nozzles are similar at 0.5l/min. Co-precipitation reaction occurs in a 50 liter vessel (6) containing NaOH 10^{-4} M to keep the reaction environment at the constant pH = 10. A reddish-brown precipitate in the colloidal paste form is obtained from this reaction. The precipitate was washed carefully then mixed with water and put into special reactor of 6 liter capacity for hydrothermal processing. Hydrothermal process was conducted at temperatures of 120^{o}C, 140^{o}C, 160^{o}C during 4 hours. Temperature was measured by a thermocouple which is mounted inside the reactor in direct contact with the slurry. After the reaction ends, the obtained brown magnetic powder has been collected by magnet and washed with distilled water before drying.

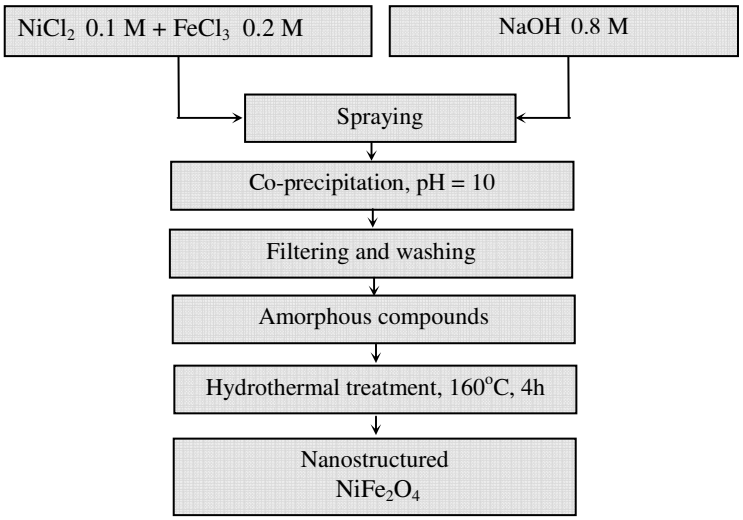

Fig. 1.a. Schematic diagram of experimental procedure.

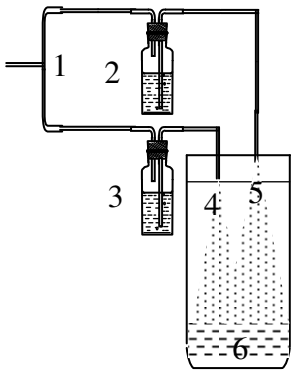

1 – Compressed air pipes

2,3 - Pressure vessel

4,5 - Compressed air sprayer

6 - Reaction vessel

Fig. 1.b. Schema of co-precipitation reaction apparatus.

2.2. Process of synthesizing the composite $NiFe_2O_4$ -TiO_2 nanoparticles.

Firstly, $TiO_2.nH_2O$ gel is synthesized from the hydrolysis of $TiCl_4$. 5.5 ml $TiCl_4$ equivalent to 5g TiO_2 and 4.8 ml Diethanolamin $NH(C_2H_4OH)_2$ were mixed in 100 ml ethanol 99.7 %. This mixed solution is frozen down to 10°C and added with 100 ml of distilled water. This solution is strongly stirred and heated until the clear milky white color appears. The reaction temperature is about 30°C at pH < 1. Then the solution NaOH 1M is slowly dropped into the mixture until pH = 7 to obtain a milky white jelly solution of TiO_2. By this time, 5 g of synthesized $NiFe_2O_4$ is added under vigorous strong stirring within 1 hour for uniform distribution of powder in the TiO_2 gel. The precipitate is filtered, washed, dried at 100°C and, finally, calcinated at 500°C for 1 hour.

2.3. Characterization of synthesized materials

For characterization of obtained materials and nanoparticles, we have used standard techniques such as XRD (Siemens D5005 with CuK_α radiation), TEM (EM 1010, JEOL), VSM (DMS 800).

2.4. Experimenting on photocatalysis of the $NiFe_2O_4$-TiO_2 composite nanoparticles.

Photocatalytic features of the $NiFe_2O_4$ - TiO_2 composite nanoparticles are studied through the process of methyl orange decomposition. Irradiation from 15W UV fluorescence lamp is used for illumination. Glass boxes containing 10ml of 10^{-4}M orange methyl and 100mg of nanocomposite material are illuminated with UV irradiation through the free surface during 2, 4, 6, 8, 10, 12, 14 hours, respectively. After illumination, nanocomposite powders are separated from the boxes by using external magnetic field. The remaining liquid shall be measured the absorption spectra on UV-VIS 2450 PC (Shimadzu, Japan) to determine the concentration of methyl orange.

3. Results and discussions

3.1. Crystallization of $NiFe_2O_4$ by hydrothermal processing

XRD pattern and TEM image of the material obtained immediately after the co-precipitation and hydrothermal processing are shown in Fig. 2 and Fig. 3, respectively. We can see that the co-precipitate is in the form of amorphous glue clusters without distinct particles, while powders obtained after hydrothermal process are single-phase crystalline $NiFe_2O_4$. TEM image in Fig. 3.b indicates shape particles with an average size of about 20 nm.

According to [7, 8], this amorphous form also contains much H_2O and only become dehydrated completely at temperature of above 600°C. We use the hydrothermal method to crystallize the amorphous material in the temperature range 120 – 160°C, which is much lower than the sintering method (600 - 1000°C).

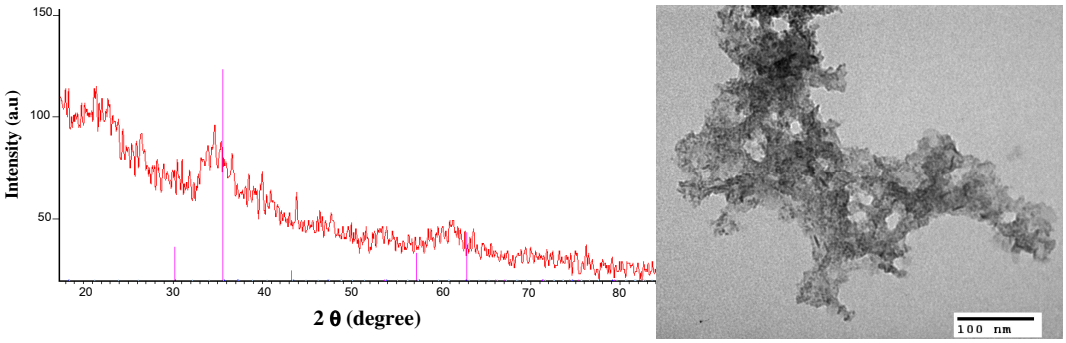

Fig. 2. XRD pattern (a) and TEM image (b) of the reddish-brown precipitate.

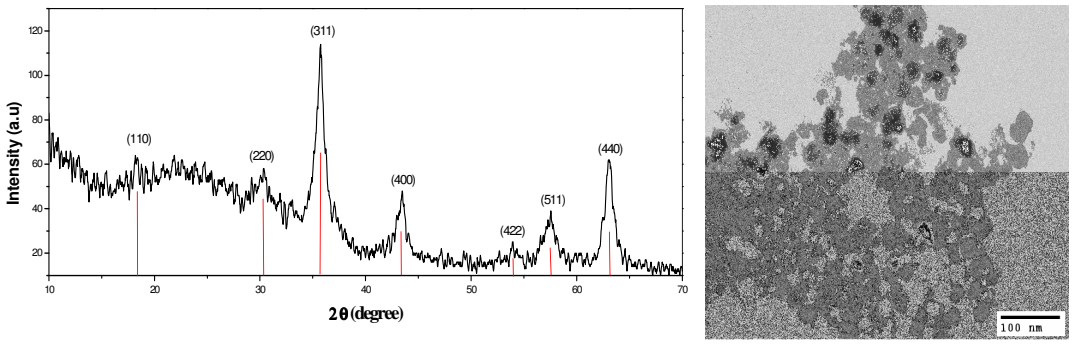

Fig. 3. XRD pattern (a) and TEM image (b) of $NiFe_2O_4$ nanoparticles prepared at hydrothermal temperature 160°C.

Therefore, it can be said that in spite of the low temperature (120 - 160°C), during the hydrothermal process under high pressure (9.5 atm), in the reactor occurs dehydration of precipitate and crystallization of $NiFe_2O_4$.

3.2. Effects of hydrothermal temperature on size and properties of $NiFe_2O_4$ nanoparticles

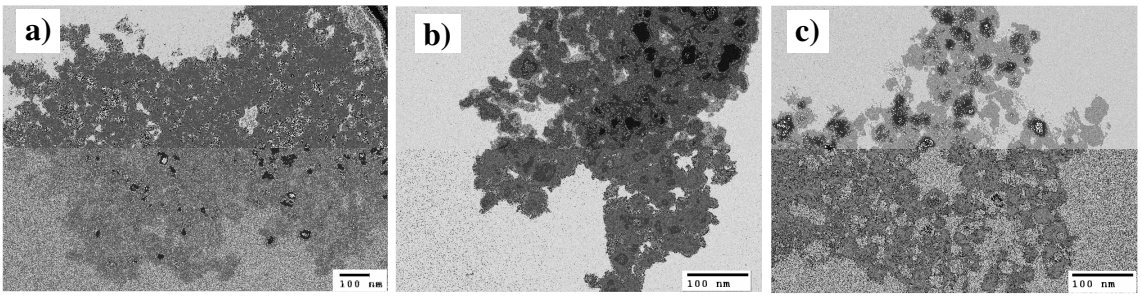

Fig. 4. TEM images of $NiFe_2O_4$ nanoparticles hydrothermalized at a)120 °C; b)140°C; c)160°C.

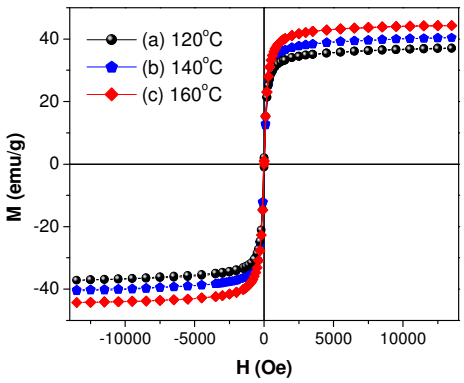

Fig. 5. Superparamagnetism of $NiFe_2O_4$ nanopowders obtained at different hydrothermal

Fig. 4 shows TEM images of $NiFe_2O_4$ nanopowders, obtained at hydrothermal temperatures of 120, 140, and 160°C, respectively. One can see that, when the hydrothermal temperature is increased, particle size and shape did not change significantly. This is understandable, because at so low temperatures, the thermal energy is not sufficient to allow small particles to assemble together into large particles.

Contrary to particle size, the magnetic properties of powders are improved remarkably when the hydrothermal temperature increases, as shown in Fig. 5. Magnetic saturation is increased significantly with increasing of hydrothermal temperature. In the region with high magnetic field, when the temperature increases, the magnetic saturation also increases from 37 emu/g (corresponding to the temperature of 120°C) to 44 emu/g (corresponding to temperature 160°C). We can see also that the powders are typically superparamagnetic with remanences (Mr) and coercive forces (Hc) being near to zero. This is very important when we want to recollect the photocatalist TiO_2 materials distributed in environment for reuse by using an external magnetic field.

3.3. Properties of anatase TiO_2 - $NiFe_2O_4$ composite nanophotocatalyst

Fig. 6 shows XRD pattern and TEM image of obtained TiO_2-$NiFe_2O_4$ composite nanoparticles. We can see typical peaks of anatase TiO_2 at diffraction angles 25°, 37°, 38°, 48°, 54°, 55°, 63° along with typical peaks of $NiFe_2O_4$. So the particles are composite of anatase TiO_2 and $NiFe_2O_4$. TEM image shows that TiO_2-$NiFe_2O_4$ nanoparticles have average particle size of 10 - 30 nm. Therefore, this material has high surface area, suitable for heterogeneous catalyst applications.

Fig. 6. XRD pattern (a)and TEM image of the nanocomposite material AnataseTiO_2 - $NiFe_2O_4$

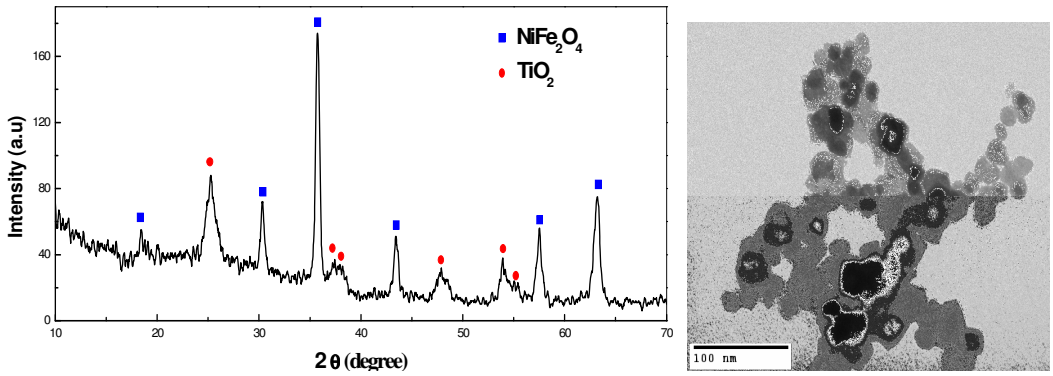

In Fig. 7 are shown results of study on photocatalytic capability of the obtained TiO_2-$NiFe_2O_4$ composite nanoparticles. Methyl orange is mixed from the standard chemical which always exists in the form of anions with pH > 7, so it can has only one color carrying form and in UV-Vis absorption spectrum it has only one characteristic absorption peak at 461 nm in accordance with [9, 10]. Fig. 7.a shows, how absorbance spectra of methyl orange solution change with UV illumination time and Fig. 7.b demonstrates the kinetics of degradation of methyl orange by composite photocatalyst under UV illumination.

We can see that the concentration of methyl orange after processing time of about 14 hours, is only 1,7. 10^{-6} M, i.e about 98,2 % of the original substance is decomposed after processing. Such the obtained composite powders show good photocatalytic properties, they can decompose effectively dye and can be used for removing other chemical in wastewater.

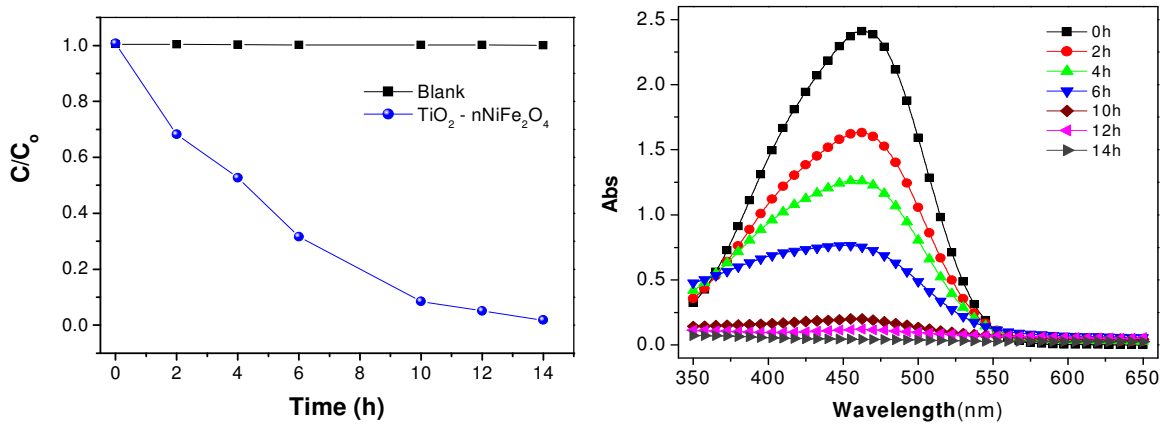

(a) **(b)**

Fig. 7. a. UV-Vis spectra of samples decomposed by time
b. Time dependence of the concentration of methyl orange in the solution

The detailed mechanism of TiO_2 catalyzed dye degradation was studied in some research [12,13]. When aqueous TiO_2 suspension is irradiated with light energy greater than its band gap energy (E_g=3.2 eV), conduction band electrons (e •) and valence band holes (h+) are generated

$$(e^-/h^+)\ TiO_2 \longrightarrow e^-(TiO_2) + h^+(TiO_2)$$

The photo-generated electrons can react with O_2 adsorbed on the TiO_2 surface or dissolved in water reducing it to superoxide radical anion O_2^-•

$$TiO_2(e^-) + O_2 \rightarrow TiO_2 + {}^{\bullet}O_2^-$$

The photo-generated holes can react with H_2O oxidizing them into OH • radicals.

$$TiO_2(h^+) + H_2O \rightarrow OH^{\bullet} + H^+ + TiO_2$$

So the role of nano TiO_2 anatase in the photocatalytic process is to transfer electrons from H_2O to O_2 . The resulting ${}^{\bullet}O_2^-$, OH • radical, being very strong oxidizing agents (OH • standard redox potential is +2.8 V), can oxidize the methyl orange dye to CO_2 and H_2O.

The major advantage of this photocatalyst is that due to the magnetic properties of $NiFe_2O_4$, the $NiFe_2O_4$-TiO_2 nanoparticles can be collected for reuse, thus bringing significant economic benefits and eliminating the risk of additional pollution source (TiO_2 solid particles) in the wastewater treatment process.

4. Conclusions

We have successfully synthesized $NiFe_2O_4$ nanoparticles with average particle size of about 20 nm by using spraying - coprecipitation process with subsequent hydrothermal treatment. Advantages of this process are very low processing temperature, high productivity, good stability and excellent superparamagnetic performances of the nanoparticles. This technological process can be easily

expanded to industrial scale for large scale production of $NiFe_2O_4$ nanoparticles and can be applied for synthesizing nanopartcles of different ferrites MFe_2O_4, as well as oxides and other materials. At the same time, we also successfully synthesized composite $NiFe_2O_4$ - TiO_2 nanoparticles, which are simultaneously good superparamagnetic and photochemical catalyst. This will facilitate the solution of problems of collection expensive TiO_2 photochemical catalyst for reuse, and also reduce the risk of contamination of TiO_2 solid waste during the environment processing.

References

[1] D.H. Han, H.L. Luo, Z. Yang, J. Magn. Magn. Mater., **161**, 376 (1996).

[2] R.A. Candeia, M.A.F. Souza, M.I.B. Bernardi, S.C. Maestrelli, I.M.G. Santos, A.G.Souza, E. Longo, Mater. Res. Bull., **41**, 183 (2006).

[3] N.Iftimie, E. Rezlescu, P.D.Popa et al, Journal optoelectronics and advance materials. **Vol. 8, No. 3**, 1016 (2006).

[4] U. Lueders, A. Bathelemy, M. Bibes et al, http://arxiv.org/abs/cond-mat/0508764.

[5] Hoffmann M.R, Martin S.T, Choi W, Bahnemann D.W, Chem. Rev., **95**, 69 (1995).

[6] Zhao J.C., Wu T.X., Wu K.Q., Oikawa K., Hidaka H., Serpone N., Environ. Sci. Technol., **32**, 2394 (1998).

[7] Jiye Fang, Narayan Shama, Le Duc Tung et al, Journal of applied physics, **Vol. 93, N.10**,7483 (2003).

[8] Santi Maensiri, Chivalrat Masingboon, Banjong Boonchom et al, Scripta Materialia, **56**, 797 (2007).

[9] Xu Sh., Shangguan W., Yuan N., Chen M. and Shi J., Chin. J. Chem. Eng, **15(2)**, 190 (2007).

[10] M.N.Rashed, A.A.El-Amin, International Journal of Physical Sciences, **Vol. 2 (3)**, 073, March, (2007).

[11] Do Quoc Hung, Dang Thi An, Advances in Natural Sciences, **Vol 8**, **No 3&4**, 469 (2007).

[12] A.R. Khataee, M.B. Kasiri, Journal of Molecular Catalysis A: Chemical, **328** pp. 8-26 (2010)

[13] Augugliaro V, Baiocchi C, Bianco Prevot A, et al, Chemosphere **49**(10): 1223-1230 (2002).